Glycobiology vol. 3 no. 3 pp. 261–269, 1993

exal 66 = GSG 1051
" 67 = " 1052
" 68 = " 1053

(4)

PubMed 8358151

Structural characterization of novel inositol phosphosphingolipids of *Tritrichomonas foetus* and *Trichomonas vaginalis*

Catherine E.Costello[1,4], John Glushka[2], Herman van Halbeek[2] and Bibhuti N.Singh[3]

[1]Mass Spectrometry Facility, Department of Chemistry, Massachusetts Institute of Technology, Cambridge, MA 02139, [2]Complex Carbohydrate Research Center and Department of Biochemistry, The University of Georgia, Athens, GA 30602 and [3]Microbiology and Immunology Department, Health Science Center, State University of New York, Syracuse, NY 13210, USA

[4]To whom correspondence should be addressed at: MIT 56-029, 77 Massachusetts Avenue, Cambridge, MA 02139, USA

Two major ethanolamine phosphate-substituted inositol phosphosphingolipids have been identified in the unsaponifiable acidic lipid fractions of *Tritrichomonas foetus* and *Trichomonas vaginalis*. The compounds were radiolabelled and purified by high-performance thin-layer chromatography followed by high-performance liquid chromatography. The structures were determined by a combination of tandem mass spectrometry (MS/MS) and nuclear magnetic resonance (NMR) experiments, and gas–liquid chromatography of components obtained by degradation and derivatization. Inositol in the *T.foetus* component was 1-linked to the phosphosphingolipid, had the phosphoethanolamine group at the 3-position and a fucosyl residue at the 4-position. The *T.vaginalis* component lacked the fucosyl moiety. Both organisms also produced inositol phosphosphingolipids having the same long-chain base (sphingosine or dihydrosphingosine) and the same fatty acyl distribution as the inositol diphosphate compounds. These glycosphingolipids may represent metabolic intermediates for new types of membrane anchors for surface glycopeptides or glycolipids that mediate the host–parasite relationship of these trichomonads. The MS/MS and NMR spectroscopic data should provide reference information for structural determinations of other phosphorylated inositol derivatives.

Key words: inositol phosphosphingolipids/NMR/tandem MS/*T.foetus*/*T.vaginalis*

Introduction

Trichomoniasis is an infection of the genitourinary tract caused by the flagellated protozoan *Trichomonas vaginalis* in humans and *Tritrichomonas foetus* in cattle. Trichomonads live on the surface of the epithelium of the urogenital tract where they derive many of their nutrients from the host, e.g. purines, pyrimidines and lipids. Until recently, lipid metabolism and the role of lipids in parasite survival in a hostile environment, surface attachment and the important involvement of glycoconjugates in these functions have been little studied in trichomonads (Holz *et al.*, 1987; Beach *et al.*, 1990, 1991; Singh *et al.*, 1991). Trichomonads are fatty acid and sterol auxotrophs (Holz *et al.*, 1987; Beach *et al.*, 1990, 1991) but they appear to synthesize glycolipids and glycophosphosphingolipids *de novo* (Singh *et al.*, 1991).

How these parasites infect and survive in the host is an intriguing problem. The surface membranes of parasitic protozoans are known to contain a variety of complex carbohydrates: glycoproteins, glycolipids and glycosylated phosphate-containing lipids. Surface glycoconjugates have been shown to be critical for the parasites' survival in the hostile immune environment of the host.

It is well accepted that glycoconjugates play a major role in phenomena such as cell–cell interaction, cell recognition, cell attachment and cell antigenicity (Hakomori, 1981; Karlsson, 1989). The surface antigens of parasites have been subject to recent major research efforts because of their important roles in parasite invasion of the host and in evasion of the host immune response (Ferguson and Homans, 1988; Turco, 1988, 1989; Greis *et al.*, 1992; Güther *et al.*, 1992; Ilg *et al.*, 1992; McConville and Homans, 1992; Thomas *et al.*, 1992).

Recently, we determined the general features of the glycophosphosphingolipids, $\mathbf{TF_1}$ and $\mathbf{TF_2}$, from *T.foetus* by using a combination of metabolic labelling, chromatography and mass spectrometric techniques (Singh *et al.*, 1991). At that time, we ascertained that $\mathbf{TF_1}$ contains an inositol phosphoceramide (the long-chain base a mixture of d18:0 and d18:1, with 16:0 as the major fatty acyl group) and that the inositol is further substituted by both fucose and phosphate, ethanolamine phosphate or *N*-acetylethanolamine phosphate. The data available at that time did not permit assignment of the inositol linkage positions. Extensive ^{1}H- and ^{31}P-NMR experiments have now confirmed the proposed structural features and have also made possible elucidation of the linkage positions of the tri-substituted inositol. This result represents a landmark for determination of the substitution pattern in a complex inositol derivative. We report here the complete structural determination of the inositol phosphosphingolipids of *T.foetus* and the characterization of parallel inositol phosphosphingolipid fractions from *T.vaginalis*, including another novel phosphoethanolamine-substituted inositol phosphosphingolipid ($\mathbf{TV_1}$).

Results

High-performance thin-layer chromatography (HPTLC) of the unsaponifiable acidic lipid fractions of *T.foetus* and *T.vaginalis* revealed two major inositol phosphosphingolipid components as determined by Dittmer–Lester reagent (Dittmer and Lester, 1964). (R_f values reported here are from the solvent system A.) These two phosphosphingolipid fractions are denoted as $\mathbf{TV_1}$ (R_f 0.35) and $\mathbf{TV_2}$ (R_f 0.51) from *T.vaginalis* and $\mathbf{TF_1}$ (R_f 0.33) and $\mathbf{TF_2}$ (R_f 0.51) from *T.foetus* (Singh *et al.*, 1991). The phosphosphingolipid $\mathbf{TV_1}$ migrated slightly ahead of $\mathbf{TF_1}$ in both solvent systems which indicated that $\mathbf{TF_1}$ could be more polar than $\mathbf{TV_1}$. These inositol phosphate-containing lipids constituted ~0.8% of *T.vaginalis* crude total lipid and 4% of *T.foetus* crude total lipid fractions. The amounts of pure

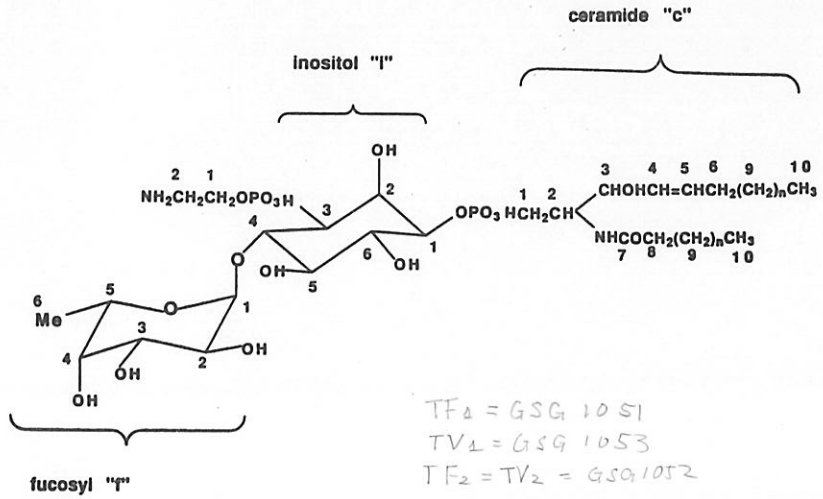

Fig. 1. Structure proposed for (the major component of) TF_1. The numbering of the carbon atoms in the different residues is used as indicated throughout the discussion of the NMR data. In TV_1, the fucosyl substituent on inositol is replaced by a hydroxyl group. TF_2 and TV_2 lack the phosphoethanolamine substituent as well, and thus have an unsubstituted phosphoinositol group.

lipid components [isolated by HPTLC followed by high-performance liquid chromatography (HPLC)] obtained were 0.5 mg of TV_1 and 0.6 mg of TV_2 from 1.82 g of crude total lipid (9.25×10^{10} cells, 22 l culture) from *T.vaginalis*, and 0.87 mg of TF_1 and 0.6 mg of TF_2 from 1.2 g of crude total lipid (11.64×10^{10} cells, 6 l culture) from *T.foetus*. [^{3}H]*myo*-Inositol and ^{32}P were incorporated into these inositol phosphosphingolipids [data not shown, results for TF_1 and TF_2 have been reported earlier (Singh *et al.*, 1991)]; however, the incorporation of these isotopes was very poor in the TV_1 and TV_2 fractions. [^{3}H]Fucose and [^{14}C]ethanolamine were also incorporated into the TF_1 fraction (Singh *et al.*, 1991). The incorporation of [^{14}C]ethanolamine into TV_1 was also very poor (data not shown).

Gas–liquid chromatographic (GLC) analysis of alditol acetates or TMS derivatives of the sugars revealed the presence of only *myo*-inositol in TV_1, TV_2 and TF_2 fractions; TF_1, however, contained both fucose and inositol (Singh *et al.*, 1991). GLC analysis of the *N*-acetyl-*O*-TMS derivatives of the ceramide long-chain bases of these phosphosphingolipids indicated mainly dihydrosphingosine and some sphingosine [(4*E*)-sphingenine]. GLC of the fatty acid methyl esters indicated that the major fatty acids were palmitic (67–70%), stearic (20%) and oleic (12–15%).

The data reported earlier (Singh *et al.*, 1991), provided from chemical analysis and tandem mass spectrometry, suggested that TF_1 contains a fucosyl- and ethanolamine phosphate-substituted inositol phosphoceramide. Larger-scale purification of this fraction and a series of ^{1}H and ^{31}P NMR experiments have now made it possible to confirm these features and to accomplish the difficult assignment of the inositol substitution sites and thereby to complete the determination of the structure illustrated in Figure 1. Crucial experiments for delineating this structure were: (i) two-dimensional (2-D) homonuclear Hartmann–Hahn spectroscopy (HOHAHA), scalar correlated spectroscopy (COSY) and rotating-frame nuclear Overhauser effect (NOE) correlated spectroscopy (ROESY) experiments to identify the spin systems of the fucosyl, inositol, ceramide and ethanolamine moieties; (ii) a 2-D long-range ^{1}H[^{31}P] scalar correlation experiment, to locate the phosphoryl groups on the inositol ring and to establish which of the two is linked to ceramide; and (iii) a 2-D ROESY experiment to ascertain a through-space connectivity between the fucosyl H1 (**f**1) and inositol H4 (**i**4) atoms.

Some assignments of the ^{1}H signals of the inositol, fucosyl, ethanolamine and ceramide groups are indicated on the full and expanded regions of the HOHAHA spectrum (Figures 2b and 3a). Additional data are found in Table I. Assignment of the fucosyl proton resonances began with the anomeric signal (**f**1) at δ 4.99 ($J_{12} < 3$ Hz, indicative of an α-L-glycosidic linkage) which shows connectivity to **f**2 through **f**4 of the ring. Proton **f**5, however, was weakly coupled to **f**4 ($J_{45} \leq 1$ Hz) and thus had a cross-peak only with the C6 methyl protons (**f**6) at 1.14 p.p.m. (see Figure 2). The corresponding region of the ROESY spectrum (Figure 4) shows a cross-peak between the fucosyl protons **f**1 and **f**2, as expected for an α-fucosyl residue, and also cross-peaks from **f**5 to **f**3 and **f**4, which share the same face of the ring.

The ceramide moiety was traced from the characteristic methine resonances at δ 5.41 and δ 5.62 (Figure 2) designated as **c**4 and **c**5 in the drawn structure (Figure 1). The non-integral intensity ratio of these two peaks (**c**4:**c**5 > 1), and the presence of more than one cross-peak between **c**4 and protons at positions **c**6 (δ 1.99 and δ 2.06), are indicative of some heterogeneity in this part of the molecule. Multiple resonances are also seen for the **c**8 protons at δ 2.09–2.15. The expanded region of the HOHAHA spectrum (Figure 3a) shows the geminal protons of **c**1, as well as protons of **c**2 and **c**3 at appropriate chemical shifts (Koerner *et al.*, 1983). The ethanolamine group has two signals at δ 3.99 and δ 3.03 (**e**1 and

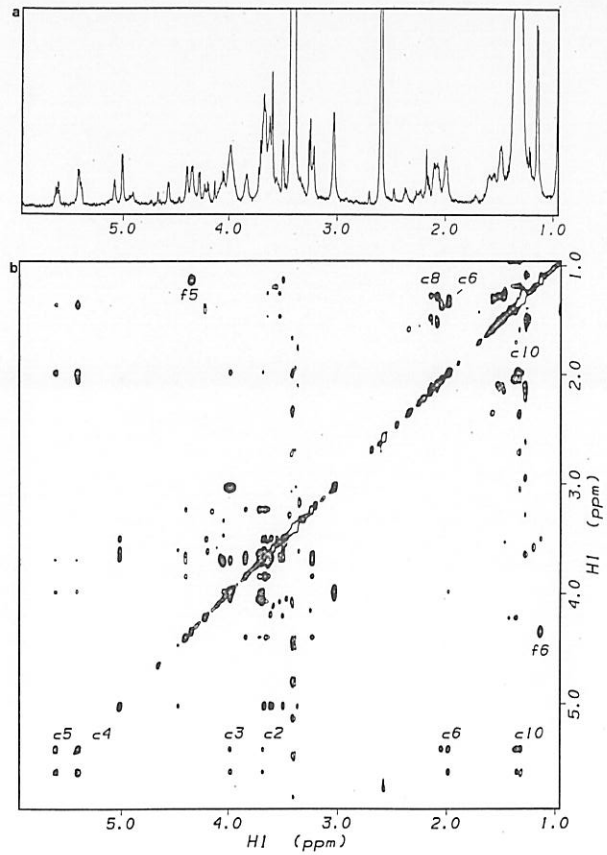

Fig. 2. (**a**) High-resolution 1-D ^{1}H-NMR spectrum of TF_1 (600 MHz, [$^2H_6$]Me_2SO, 23°C). (**b**) Two-dimensional HOHAHA spectrum of TF_1 (600 MHz, [$^2H_6$]Me_2SO, 23°C).

e2, respectively); a minor pair of correlated peaks observed at δ 4.04 and δ 3.71 is probably due to **e**1 and **e**2 in *N*-acetylethanolamine.

The inositol spin system could be traced, but assignment of the signals was more difficult. The substitution pattern of the inositol was not evident from the chemical shifts of its ring protons. Typically, in unsubstituted *myo*-inositol, the single equatorial proton at position 2 (**i**2) resonates ~0.5 p.p.m. or more downfield than the axial proton signals, while the axial proton at position **i**5, directly opposite to **i**2, is found relatively upfield (Johansson *et al.*, 1990). Substitution of hydroxyl groups, however, can alter this arrangement. The assignment presented for the inositol residue in TF_1 (Table I) was based on the pattern described above, i.e. the signals at δ 4.42 and δ 3.23 were attributed to **i**2 and **i**5, respectively. The complete spin system was traceable from either **i**2 or **i**5 in the HOHAHA spectrum (Figure 3a). The direction of numbering for the remaining protons was based on the substitution pattern of the inositol ring discussed below. From the double-quantum-filtered (DQF)-COSY spectrum of TF_1 (data not shown), **i**5 is connected to two signals (**i**6 and **i**4) at δ 3.66 and δ 3.71, respectively. The downfield member of this pair is connected to **i**3 at δ 3.85. The equatorial proton at **i**2 does not show any connectivity in the COSY spectrum, but from the HOHAHA data, the remaining inositol peak at δ 3.63 was assigned to **i**1. The ROESY spectrum shows expected cross-peaks (not seen at levels displayed in Figure 4) between **i**5, **i**3 and **i**1, which feature a tri-axial spin system on the same face of the inositol ring.

The position of the fucosyl linkage was determined to be (1→4), based on a strong NOE between the anomeric proton **f**1 and **i**4 (Figure 4). The mass spectral data showed that the ethanolamine and ceramide groups were connected via phosphoryl groups, and an ^{1}H[^{31}P] correlated spectrum supported this conclusion. The spectrum (see Figure 3b) showed two signals in the ^{31}P dimension at δ −0.34 and δ −1.76 p.p.m.,

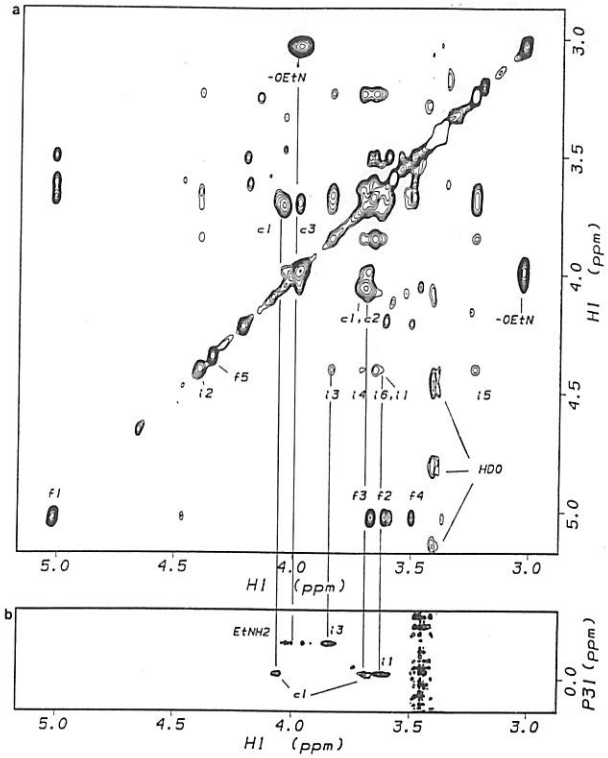

Fig. 3. (a) Expanded region of the 2-D HOHAHA spectrum of $\mathbf{TF_1}$ (see Figure 2b). (b) Corresponding region of the 2-D $^1H[^{31}P]$-HMQC spectrum of $\mathbf{TF_1}$ (500 MHz, $[^2H_6]Me_2SO$, 23°C).

both characteristic of phosphodiesters (Tebby, 1987). The downfield ^{31}P signal is correlated to the **c**1 geminal protons of the ceramide group and also to the proton assigned to i1 of the inositol. The second ^{31}P signal is correlated to i3 and weakly to a multiplet signal that has a position similar to the ethanolamine resonances at δ 3.99–4.04. Thus, by NMR, the phosphate groups and the fucosyl residue were located on the *myo*-inositol i1, i3 and i4 positions, respectively. However, it should be mentioned that it was proposed that the sample also contains compounds in which the ethanolamine is lacking, or is *N*-acetylated. This heterogeneity is reflected in the presence of additional peaks in the NMR spectra, some of which could not be fully analysed.

The liquid secondary ion mass spectrometry (LSIMS) and collision-induced dissociation tandem mass spectrometry (CID MS/MS) spectra of $\mathbf{TV_1}$ indicate that it has a structure related to that of $\mathbf{TF_1}$, but lacks fucose. The $(M\text{-}H)^-$ of the major component was observed at *m/z* 903.6 (146 u lower than that of $\mathbf{TF_1}$) and the less abundant component at *m/z* 901.6, the abundance ratio of the $(M\text{-}H)^-$ ions being ~2.5:1. The CID mass spectrum of *m/z* 903.6 (Figure 5) could be interpreted (Scheme 1) by analogy to the assignments proposed previously for the CID MS/MS spectrum of the $\mathbf{TF_1}$ $(M\text{-}H)^-$ (Singh *et al.*, 1991). Losses of 43 and 123 u from the molecular ion corresponded to expulsion of CH_2CH_2NH and $HPO_3CH_2CH_2NH$, respectively. Cleavage of the inositol–phosphate bond yielded the Y_0PO_3H fragment containing the phosphoceramide at *m/z* 618.5; cleavage of the ceramide–phosphate bond yielded the C_1PO_3H fragment containing ethanolamine phosphate-substituted phosphoinositol at *m/z* 382.0 [for designations of the fragment ions, see Costello and Vath (1990)]. Observation of the U fragment at *m/z* 661.4 indicated that the long-chain base was dihydrosphingosine and the 16:0 fatty acyl group was present. Consistent with this assignment, the CID mass spectrum of *m/z* 618.6 (not shown) had an abundant U fragment at *m/z* 376.1.

A very minor component of $\mathbf{TV_1}$ had $(M\text{-}H)^-$ *m/z* 1049.8 and a CID spectrum like that obtained for the ion at this mass in the $\mathbf{TF_1}$ spectrum. This minor component was therefore assumed to be the fucosylated analogue.

The negative-ion LSIMS mass spectrum of $\mathbf{TV_2}$, shown in Figure 6, corresponded to the inositol phosphate ceramide, with

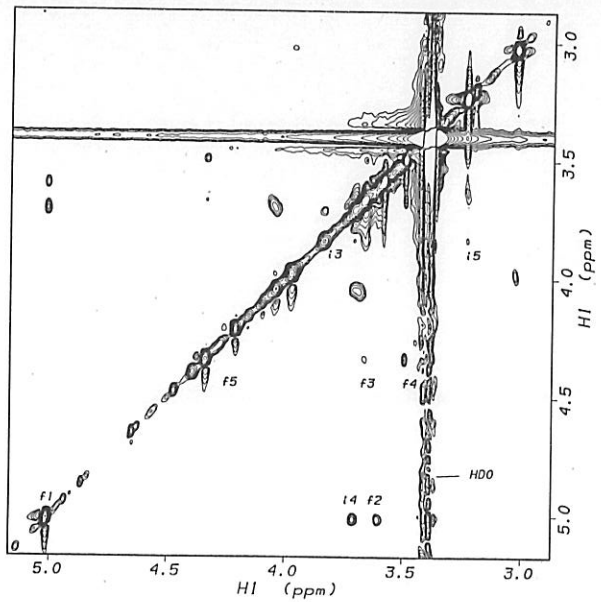

Fig. 4. Expanded region of the 2-D $[^1H,^1H]$ ROESY spectrum of $\mathbf{TF_1}$ (600 MHz, $[^2H_6]Me_2SO$, 23°C), corresponding to the HOHAHA spectrum in Figure 3a.

Table I. ^1H chemical shifts for aliphatic protons in $\mathbf{TF_1}$

	Chemical shift[a] in residue			
Proton	**f** (fucosyl)	**i** (inositol)	**e** (ethanolamine)	**c** (ceramide)
H1	4.99	3.63	3.99	4.06
H1′				3.7[b]
H2	3.60	4.42	3.03	3.69
H3	3.67	3.85		3.98
H4	3.50	3.71		5.41
H5	4.33	3.23		5.62
H6	1.14	3.66		2.06
H6′				1.99
H8				2.15
H8′				2.09
H9				1.30–1.33[c]
H10				0.93[d]
$NCOCH_3$			2.16[e]	

[a]Data were acquired for a solution of $\mathbf{TF_1}$ in $[^2H_6]Me_2SO$ at 600 MHz and 23°C. Chemical shifts are referenced to internal sodium 4,4-dimethyl-4-silapentane-1-sulphonate (DSS), with residual $[^2H_5]Me_2SO$ as the internal standard at δ 2.58 p.p.m.
[b]Chemical shift cannot be specified in greater detail due to the higher-order pattern.
[c]All methylene H9 signals are found between δ 1.30 and 1.33 p.p.m.
[d]Signal due to six protons.
[e]Tentative assignment.

$(M\text{-}H)^-$ *m/z* 780.6, fragment Y_0PO_3H at *m/z* 618.6 and the phosphoinositol anion at *m/z* 258.9. Its general structure is, therefore, the same as $\mathbf{TF_2}$, the difference being only in the ratio of the long-chain bases; $\mathbf{TV_2}$ contains relatively more dihydrosphingosine, but both have predominantly the 16:0 fatty acyl group.

Discussion

Trichomonas vaginalis and *T.foetus* each contain two major glycophosphosphingolipids, designated $\mathbf{TV_1}$ and $\mathbf{TV_2}$, and $\mathbf{TF_1}$ and $\mathbf{TF_2}$, respectively, which can be metabolically labelled with $[^3H]$*myo*-inositol and $H_3{}^{32}PO_4$. $\mathbf{TF_1}$ of *T.foetus* could be preferentially radiolabelled with $[^3H]$fucose and $[^{14}C]$ethanolamine, as reported earlier (Singh *et al.*, 1991). Both lipids from *T.vaginalis* and *T.foetus* contain ceramides. The major long-chain base in both is dihydrosphingosine (d18:0); sphingosine (d18:1) is also present and the 16:0 *N*-acyl group is the most abundant. $\mathbf{TV_1}$, like $\mathbf{TF_1}$, contains an ethanolamine-substituted inositol phosphoceramide. To our knowledge there are no other accounts of similarly substituted compounds. The present work employed several NMR techniques to confirm our initial assignment of the *T.foetus* inositol diphosphate fraction $\mathbf{TF_1}$ and to complete the structural determination by adding positional information on the three inositol substitution sites.

The investigations have also shown that the lipid fractions $\mathbf{TF_2}$ and $\mathbf{TV_2}$ contain inositol phosphosphingolipids. The chromatographic and mass spectral data are quite definitive on these points. We have determined the structures of other inositol phospholipids of *T.foetus* and *T.vaginalis*, and have found them to be glyceride and diglyceride esters (Costello *et al.*, 1990).

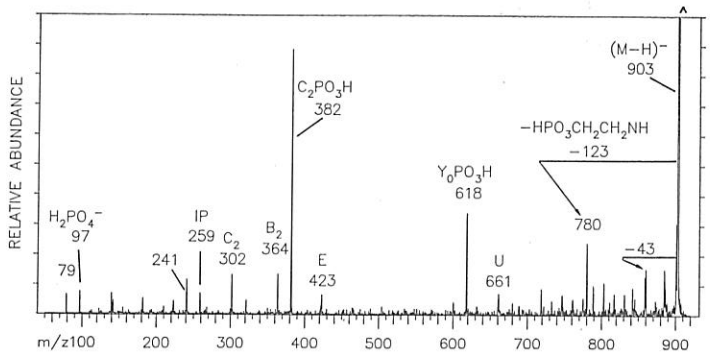

Fig. 5. CID MS/MS spectrum of the $(M-H)^-$, *m/z* 903.6, in the LSIMS mass spectrum of $\mathbf{TV_1}$. Fragment ion assignments are shown in Scheme 1. IP = inositol phosphate.

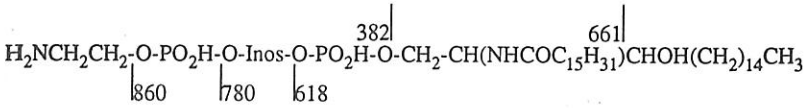

Scheme I

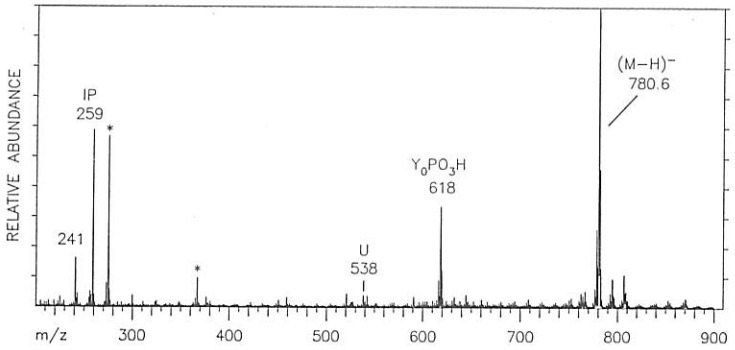

Fig. 6. Negative-ion LSIMS mass spectrum of $\mathbf{TV_2}$ dissolved in chloroform/methanol with glycerol matrix. Fragment ion assignments are shown in Scheme 2. IP = inositol phosphate; * indicates matrix cluster ion.

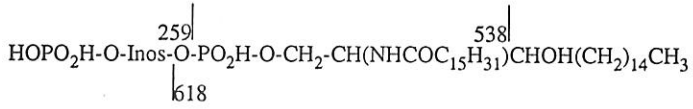

Scheme II

Lipid metabolism in trichomonads has been little studied, but is clearly defective. The poor incorporation of radiolabelled orthophosphate, inositol and ethanolamine precursors into glycosphingolipids by *T.vaginalis* is not well understood. Our studies have demonstrated poor incorporation of radiolabelled ^{32}P, inositol and ethanolamine precursors into most phosphoglycerides, a result which suggests a major impairment in synthesis. Phospholipid, fatty acid and sterol metabolism of cultured *T.foetus* and *T.vaginalis* has been investigated (Beach *et al.*, 1990, 1991). For the most part, they observed that radiolabelled precursors were even less well incorporated into the expected phospholipids of *T.vaginalis*, which may suggest that these cells have a greater deficiency in the biosynthesis of phosphoglycerides and perhaps also in glycophosphosphingolipids.

The glycosylated phosphatidyl inositol (GPI) glycolipids have been detected as membrane anchors for a wide variety of eukaryotic proteins, where these anchors are conjugated to the protein C-terminus through an amide bond to ethanolamine which is linked by a phosphodiester bond to an oligosaccharide (Low, 1989; Cross, 1990). There is some evidence that certain protozoans have glycoconjugates anchored uniquely by a ceramide moiety. This type of structure has been suggested for *Dictyostelium discoideum* adhesion proteins (Stadler *et al.*, 1989), lipopeptidophosphoglycan from *Trypanosoma cruzi* (Previato *et al.*, 1990) and lipophosphoglycan from *Acanthamoeba castellani* (Dearborn *et al.*, 1976).

$\mathbf{TF_1}$ and $\mathbf{TV_1}$ appear to be a novel class of glycophosphosphingolipids, which may be intermediates in the biosynthesis of membrane anchor proteins or other glycoconjugates to trichomonads. Our recent studies on lipophosphoglycan-like glycoconjugates from *T.foetus* indicate the presence of large amounts of fucose in the lipophosphoglycan-like molecules (Singh, 1993). This lends support to our hypothesis that compounds such as $\mathbf{TF_1}$ may be intermediates in the biosynthesis of such complex glycoconjugates. Our results further indicate that the lipophosphoglycans of both *T.foetus* and *T.vaginalis* are ceramide-containing lipids (B.N.Singh, D.H.Beach and C.E.Costello, manuscript in preparation). The set of compounds discussed here are probably further examples of the structural diversity employed by various organisms to provide membrane surface anchor sites.

Materials and methods

Materials

Sephadex G-25 and DEAE Sephadex A-25 were from Pharmacia and Iatrobead (GRS-8060) silicic acid was from Iatron Lab, Tokyo. Pre-coated HPTLC (0.2 mm thickness) plates were purchased from Merck. [2-^{14}C]Ethanolamine HCl (43 Ci/mmol) and *myo*-[2-^{3}H]inositol (13 Ci/mmol) were from Amersham Corp., and L-[5,6-^{3}H] fucose (60 Ci/mol) was from American Radiolabeled Chem. Inc. [^{32}P]Orthophosphoric acid (carrier free) was purchased from New England Nuclear. All other reagents were of the highest purity commercially available.

Cell culture

Tritrichomonas foetus strain KV_1 (ATCC 30924) and *T.vaginalis* strain CD-C85 (ATCC 50143) were grown in Diamond's medium (Diamond, 1968) with 10% heat-inactivated fetal calf serum (Hyclone Labs, Inc.) at 37°C in screw-capped 100 ml and 500 ml serum bottles, in 100–500 ml amounts. The initial pH was 7.2 for *T.foetus* and 6.2 for *T.vaginalis*, and the inoculum was 1×10^6 cells/ml. Organisms were counted at 24 h (Coulter Counter, Model Z_F, Coulter Electronics), harvested by centrifugation (6000 *g*) and washed twice in cold, phosphate-buffered saline.

Isolation and purification of glycosyl inositol phosphosphingolipids

Cells were extracted twice sequentially with 20 vols of chloroform/methanol/water (C/M/W) (30:60:8) followed by C/M/W (120:60:9) and C/M/W (10:10:3). Samples were sonicated (20–30 s) in the first extraction solvent mixture with a high-intensity ultrasonic processor equipped with a tapered microtip (Model VC 500, Sonics and Materials, Inc.). The extracts were pooled and evaporated to dryness under reduced pressure. The residue was dissolved in C/M/W (120:60:9) and lipids were separated from non-lipid contaminants and salt by Sephadex G-25 column chromatography as described by Guo *et al.* (1989). In some experiments, the extracted lipid mixture was saponified with 0.35 M KOH in methanol and neutralized as described previously (Singh *et al.*, 1991) prior to Sephadex G-25 column chromatography. Inositol phosphate-containing lipids were separated from the neutral glycolipid fraction by DEAE Sephadex A-25 column chromatography and inositol phosphate-containing lipids were further purified as reported earlier (Singh *et al.*, 1991). Thin-layer chromatography was performed using the following solvent systems: A, chloroform/methanol/0.05% $CaCl_2$ (55:40:10); B, C/M/W (60:35:8). Inositol phosphate glycolipids were detected on HPTLC by spray reagents: Dittmer–Lester for phosphate and orcinol–H_2SO_4 for sugars. Lipids radiolabelled with ^{14}C and ^{32}P were detected by TLC autoradiography on Kodak X-Omat AR film directly exposed to TLC plates. Tritiated components were detected by fluorography at −75°C, with the film exposed to the plates presprayed with EN^{3}HANCE (NEN). Initially, the lipid components were separated on HPTLC in solvent system A. Individual glycolipid bands were recovered by scraping and extracted from the silica gel by sonication with C/M/W (45:45:10) followed by C/M/W (88:44:7) twice prior to HPLC.

HPLC purification of inositol phosphate-containing glycolipids

The inositol phosphate-containing glycolipids eluted from the Iatrobead silicic acid column followed by HPTLC were further purified by HPLC (Waters) employing a (4.6 × 150 mm) Iatrobead column (6RS-8010, Iatron Lab., Tokyo) as described earlier (Singh *et al.*, 1991). Briefly, the lipids were eluted using a linear C/M/W gradient (75:24:1→50:42:8). The flow rate was 1.5 ml/min and fractions were collected at 2 min intervals. Each fraction was analysed by HPTLC in solvent system A. Fractions 3–6 (containing $\mathbf{TF_2}$ or $\mathbf{TV_2}$) and 11–20 (containing $\mathbf{TV_1}$) or 13–22 (containing $\mathbf{TF_1}$) were pooled and dried under N_2.

Analysis of the ceramide moiety

Glycolipid samples (150–200 μg) were hydrolysed with HCl in the presence of methanol and water (3:27:6) at 75°C for 18 h. Liberated fatty acid methyl esters and long-chain bases were separated and analysed by GLC as reported previously (Singh *et al.*, 1987).

Inositol analysis by GLC

Glycolipid samples were hydrolysed with 6 M HCl in the presence of Tris–HCl (3 μmol), to improve inositol recovery (Roberts *et al.*, 1987), at 110°C for 16 h. The samples were dried and then derivatized with *N,O-bis*(trimethylsilyl) trifluoroacetamide/trimethylchlorosilane/pyridine (10:1:10) for 2 h at room temperature. Samples were dried under N_2 and dissolved in hexane. Aliquots of the mixture were analysed on a Hewlett-Packard Model HP 5790A GC equipped with a (30 m × 0.32 mm) SPB-1 column (Supelco, Inc.), 175–260°C temperature programmed at 4°C/min, flame ionization detector.

GLC analysis of alditol acetates

Samples were hydrolysed with 2.5 N trifluoroacetic acid for 4 h at 100°C under N_2. The reaction mixture was cooled and dried under N_2, followed by reduction and acetylation as described earlier (Singh *et al.*, 1991). Alditol acetates were analysed on a Hewlett-Packard Model 5790A GC equipped with a (30 m × 0.32 mm) SP 2330 (Supelco, Inc.) column, temperature programmed from 220 to 240°C at 5°C/min, flame ionization detector.

LSIMS and CID MS/MS

Samples for LSIMS were dissolved (2–5 μg/μl) in choroform/methanol (2:1) and 0.3 μl of this solution was mixed 1:1 with the matrix (glycerol for positive-ion spectra, *N,N,N*-triethanolamine for negative-ion spectra). LSIMS spectra were recorded using MS-1 of a JEOL HX110/HX110 tandem mass spectrometer, fitted with a JEOL high-voltage Cs^+ gun, operated at 25 kV for positive-ion spectra and a JEOL FAB gun, operated at 6 kV with Xe^0, for negative-ion spectra. CID MS/MS spectra were acquired using all four sectors of the instrument, which has E_1B_1–E_2B_2 configuration with a collision cell

located between MS-1 and MS-2. The collision gas was He, at a pressure sufficient to reduce the precursor abundance to 25% of its initial value. The cell was floated at 3 kV with respect to ground, so that collisions took place at 7 keV. In both MS-1 and MS-2, the accelerating voltage was ±10 kV and 18–20 kV post-acceleration were applied at the detectors. MS-1 was operated at or above unit resolution. MS-2 resolution was 1:1000. Instrument operation and data acquisition were carried out by the JEOL DA-5000 data system. MS-1 spectra were acquired during scans of the magnetic field and MS-2 spectra during linked scans of the magnetic and electric fields at constant B/E ratio.

NMR spectroscopy

A sample of $\mathbf{TF}_1$ (~1 mg) was dissolved in [$^2H_6$]Me_2SO, after exchange with deuterium oxide. ^{1}H-NMR spectra were recorded at 600 MHz on a Bruker AMX-600 spectrometer at 23 or 32°C. ^{31}P-NMR data were collected at 202.5 MHz on a Bruker AM-500 spectrometer at 23°C. Two-dimensional DQF-COSY (Piantini *et al.*, 1982), HOHAHA (Bax and Davis, 1985a), ROESY (Bax and Davis, 1985b) and ^{1}H[^{31}P]-heteronuclear multiple-quantum coherence spectroscopy (HMQC) (Bax *et al.*, 1983) experiments were performed in phase-sensitive mode using the time-proportional phase incrementation (TPPI) (Marion and Wüthrich, 1983) method. Typically, 512 free induction decays (FIDs) of 2048 complex points were acquired. In all experiments, low-power presaturation was applied to the residual HDO signal. The spectral width was set to 6024 Hz for the homonuclear experiments at 600 MHz. The HOHAHA pulse program used a 130 ms, MLEV-17 (Bax and Davis, 1985a) spin-lock mixing pulse. The ROESY sequence contained a 200 ms, 2.6 kHz continuous spin-lock that was offset by 1500 Hz from the carrier placed at the residual HDO signal. Flanking 90° pulses (Griesinger and Ernst, 1987) were added for offset compensation. The ^{1}H[^{31}P]-HMQC experiment was conducted in the inverse mode, with the ^{1}H spectral width set to 3496 Hz. The ^{31}P transmitter was placed at 202.46 MHz, near the ^{31}P resonance of 85% H_3PO_4 which served as an external reference for ^{31}P chemical shifts. No decoupling was applied during data acquisition. A total of 128 FIDs of 2048 complex points were acquired. All NMR spectra were processed off-line using the FELIX 2.0 software package (Hare Research, Bothel, WA) on either SUN-4 or SGI work stations.

Acknowledgements

This research was supported by National Institutes of Health Grants P41-RR-00317 (to K.Biemann), R01-AI-29751 (to H.v.H.), P41-RR-05351 (to H.v.H.), S10-RR-04720 (to H.v.H.) and R01-AI-36680 (to G.Lindmark). Preliminary accounts of some aspects of this investigation were presented at the 38th ASMS Conference on Mass Spectrometry and Allied Topics, Tucson, AZ, June 1990, and the 11th International Symposium on Glycoconjugates, Toronto, Canada, July 1991 (abstract, *Glycoconjugate J.*, **8**, 242–243).

Abbreviations

CID, collision-induced dissociation; COSY, scalar correlated spectroscopy; 1-D, 2-D, one-dimensional, two-dimensional; DQF, double-quantum-filtered; DSS, sodium 4,4-dimethyl-4-silapentane-1-sulphonate; FID, free induction decay; Fuc, L-fucose; GC/MS, gas chromatography–mass spectrometry; GPI, glycosylated phosphatidyl inositol; HMQC, heteronuclear multiple-quantum coherence spectroscopy; HOHAHA, homonuclear Hartmann–Hahn spectroscopy; HPLC, high-performance liquid chromatography; HPTLC, high-performance thin-layer chromatography; LSIMS, liquid secondary ion mass spectrometry; MLEV, composite pulse sequence introduced by Malcolm Levitt; MS/MS, tandem mass spectrometry; myo-In, *myo*-inositol; NOE, nuclear Overhauser effect; ROE, nuclear Overhauser effect in the rotating frame; ROESY, rotating-frame NOE correlated spectroscopy; TPPI, time-proportional phase incrementation.

References

Bax,A. and Davis,D.G. (1985a) MLEV-17-based two-dimensional homonuclear magnetization transfer spectroscopy. *J. Magn. Reson.*, **65**, 355–360.

Bax,A. and Davis,D.G. (1985b) Practical aspects of two-dimensional transverse NOE spectroscopy. *J. Magn. Reson.*, **63**, 207–213.

Bax,A., Griffey,R.H. and Hawkins,B.L. (1983) Correlation of proton and nitrogen-15 chemical shifts by multiple quantum NMR. *J. Magn. Reson.*, **55**, 301–315.

Beach,D.H., Holz,G.G.,Jr, Singh,B.N. and Lindmark,D.G. (1990) Fatty acid and sterol metabolism of cultured *Trichomonas vaginalis* and *Tritrichomonas foetus*. *Mol. Biochem. Parasitol.*, **38**, 175–190.

Beach,D.H., Holz,G.G.,Jr., Singh,B.N. and Lindmark,D.G. (1991) Phospholipid metabolism of cultured *Trichomonas vaginalis* and *Tritrichomonas foetus*. *Mol. Biochem. Parasitol.*, **44**, 97–108.

Costello,C.E. and Vath,J.E. (1990) Tandem mass spectrometry of glycolipids. *Methods Enzymol.*, **193**, 738–770.

Costello,C.E., Zeng,C.-H., Beach,D.H. and Singh,B.N. (1990) *Abstracts of the 39th American Society for Mass Spectrometry Conference*, Tucson, AZ, June 1990, pp. 1403–1404.

Cross,G.A.M. (1990) Glycolipid anchoring of plasma membrane proteins. *Annu. Rev. Cell Biol.*, **6**, 1–39.

Dearborn,D.G., Smith,S. and Korn,E.D. (1976) Lipophosphoglycan of the plasma membrane of *Acanthamoeba castellani*. *J. Biol. Chem.*, **251**, 2976–2982.

Diamond,L.D. (1968) Techniques of axenic culture of *Entamoeba histolytica* Schandin 1903 and *E. histolytica*-like amoeba. *J.Parasitol.*, **54**, 1047–1056.

Dittmer,J.C. and Lester,R.L. (1964) A simple, specific spray for the detection of phospholipids on thin-layer chromatography. *J. Lipid Res.*, **5**, 126–127.

Ferguson,J.A.J. and Homans,S.W. (1988) Parasite glycoconjugates: towards the exploitation of their structure. *Parasite Immunol.*, **10**, 465–479.

Greis,K.D., Turco,S.J., Thomas,J.R., McConville,M.J., Homans,S.W. and Ferguson,M.A.J. (1992) Purification and characterization of an extracellular phosphoglycan from *Leishmania donovani*. *J. Biol. Chem.*, **267**, 5876–5881.

Griesinger,C. and Ernst,R.R. (1987) Frequency offset effects and their elimination in NMR rotating-frame cross-relaxation spectroscopy. *J. Magn. Reson.*, **75**, 261–271.

Guo,N., Her,G.R., Reinhold,V.N., Brennan,N.J., Siraganian,R.P. and Ginsburg,V. (1989) Monoclonal antibody AA4, which inhibits binding of IgE to high affinity receptors on rat basophilic leukemia cells, binds to novel α-galactosyl derivatives of ganglioside G_{D1b}. *J. Biol. Chem.*, **264**, 13267–13272.

Güther,M.L.S., Cardoso de Almeida,M.L., Yoshida,N. and Ferguson, M.A.J. (1992) Structural studies on the glycosylphosphatidylinolitol membrane anchor of *Trypanosoma cruzi*. *J. Biol. Chem.*, **267**, 6820–6828.

Hakomori,S.I. (1981) Glycosphingolipids in cellular interaction, differentiation and oncogenesis. *Annu. Rev. Biochem.*, **50**, 733–764.

Holz,G.G.,Jr, Lindmark,D.G., Beach,D.H., Neale,K.A. and Singh,B.N. (1987) Lipids and lipid metabolism of trichomonads. *Acta Univ. Carol. Biol. Prague*, **30**, 299–311.

Ilg,T., Etges,R., Overath,P., McConville,M.J., Thomas-Oates,J., Thomas,J., Homans,S.W. and Ferguson,M.A.J. (1992) Structure of the *Leishmania mexicana* lipophosphoglycan. *J. Biol. Chem.*, **267**, 6834–6840.

Johansson,C., Kordel,J. and Drakenberg,T. (1990) Analysis of myoinositol phosphates by 2D ^{1}H-n.m.r. spectroscopy. *Carbohydr. Res.*, **207**, 177–183.

Karlsson,K.-A. (1989) Glycosphingolipids as membrane attachment sites for bacteria. *Annu. Rev. Biochem.*, **58**, 309–350.

Koerner,T.A.W.,Jr, Prestegard,J.H., Demou,P.C. and Yu,R.K. (1983) High-resolution proton-NMR studies of gangliosides. 1. Use of homonuclear two-dimensional spin-echo *J*-correlated spectroscopy for determination of residue composition and anomeric configurations. *Biochemistry*, **22**, 2676–2686.

Low,M.G. (1989) The glycosyl-phosphatidylinositol anchor of membrane proteins. *Biochim. Biophys. Acta*, **977**, 427–454.

Marion,D. and Wüthrich,K. (1983) Application of phase sensitive two-dimensional correlated spectroscopy (COSY) for measurements of ^{1}H-^{1}H spin-spin coupling constants in proteins. *Biochem. Biophys. Res. Commun.*, **113**, 967–974.

McConville,M.J. and Homans,S.W. (1992) Identification of defect in lipophosphoglycan biosynthesis in a non-pathogenic strain of *Leishmania major*. *J. Biol. Chem.*, **267**, 5855–5861.

Piantini,U., Sørensen,O.W. and Ernst,R.R. (1982) Multiple quantum filters for elucidating NMR coupling networks. *J. Am. Chem. Soc.*, **104**, 6800–6801.

Previato,J.O., Gorin,P.A.J., Mazurek,M., Xavier,M.T., Fournet,B., Wieruszeski,J.M. and Mendança-Previato,L. (1990) Primary structure of oligosaccharide chain of lipopeptidophosphoglycan of epimastigote forms of *Trypanosoma cruzi*. *J. Biol. Chem.*, **265**, 2518–2526.

Roberts,W.L., Kim,B.H. and Rosenberry,T.L. (1987) Differences in the glycolipid membrane anchors of bovine and human erythrocyte acetylcholinesterases. *Proc. Natl. Acad. Sci. USA*, **84**, 7817–7821.

Singh,B.N. (1993) The lipophosphoglycan-like glycoconjugates of *Tritrichomonas foetus* and *Trichomonas vaginalis*. *Mol. Biochem. Parasitol.*, in press.

Singh,B.N., Costello,C.E., Levery,S.B., Walenga,R.W., Beach,D.H., Mueller,J.F. and Holz,G.G.,Jr (1987) Tegument galactosylceramides of the cestode *Spirometra mansonoides*. *Mol. Biochem. Parasitol.*, **26**, 99–112.

Singh,B.N., Costello,C.E. and Beach,D.H. (1991) Structures of glycophosphosphingolipids of *Tritrichomonas foetus*. *Arch. Biochem. Biophys.*, **286**, 409-418.

Stadler,J., Keenan,T.W., Bauer,G. and Gerisch,G. (1989) The contact site A glycoprotein of *Dictyostelium discoideum* carries a phospholipid anchor of a novel type. *EMBO J.*, **8**, 371–377.

Tebby,J.C. (1987) General experimental techniques and compilation of chemical shift data. In Verkade,J.G. and Quin,L.D. (eds), *Methods in Stereochemical Analysis, Volume 8: Phosphorus-31 NMR Spectroscopy in Stereochemical Analysis: Organic Compounds and Metal Complexes*. VCH Publishers, New York, p. 33.

Thomas,J.R., McConville,M.J., Thomas-Oates,J.E., Homans,S.W., Ferguson, M.A.J., Gorin,P.A.J., Greis,K.D. and Turco,S.J. (1992) Refined structure of lipophosphoglycan of *Leishmania donovani*. *J. Biol. Chem.*, **267**, 6829–6833.

Turco,S.J. (1988) The lipophosphoglycan of *Leishmania*. *Parasitol. Today*, **4**, 255–257.

Turco,S.J. (1990) The leishmanial lipophosphoglycan: a multifunctional molecule. *Exp. Parasitol.*, **70**, 241–245.

Received on December 30, 1992; accepted on March 8, 1993